

NEUTRON STAR MERGERS AS THE ORIGIN OF r -PROCESS ELEMENTS IN THE GALACTIC HALO BASED ON THE SUB-HALO CLUSTERING SCENARIO

YUHRI ISHIMARU^{1,3}, SHINYA WANAJO², AND NIKOS PRANTZOS³

Draft version June 19, 2021

ABSTRACT

Binary mergers (NSMs) of double neutron star (and black hole–neutron star) systems are suggested to be major sites of r -process elements in the Galaxy by recent hydrodynamical and nucleosynthesis studies. It has been pointed out, however, that the estimated long lifetimes of neutron star binaries are in conflict with the presence of r -process-enhanced halo stars at metallicities as low as $[\text{Fe}/\text{H}] \sim -3$. To resolve this problem, we examine the role of NSMs in the early Galactic chemical evolution on the assumption that the Galactic halo was formed from merging sub-halos. We present simple models for the chemical evolution of sub-halos with total final stellar masses between $10^4 M_\odot$ and $2 \times 10^8 M_\odot$. Typical lifetimes of compact binaries are assumed to be 100 Myr (for 95% of their population) and 1 Myr (for 5%), according to recent binary population synthesis studies. The resulting metallicities of sub-halos and their ensemble are consistent with the observed mass-metallicity relation of dwarf galaxies in the Local Group, and the metallicity distribution of the Galactic halo, respectively. We find that the r -process abundance ratios $[r/\text{Fe}]$ start increasing at $[\text{Fe}/\text{H}] \leq -3$ if the star formation efficiencies are smaller for less massive sub-halos. In addition, the sub-solar $[r/\text{Fe}]$ values (observed as $[\text{Ba}/\text{Fe}] \sim -1.5$ for $[\text{Fe}/\text{H}] < -3$) are explained by the contribution from the short-lived (~ 1 Myr) binaries. Our results indicate that NSMs may have a substantial contribution to the r -process element abundances throughout the Galactic history.

Subject headings: nuclear reactions, nucleosynthesis, abundances — Galaxy: evolution — Galaxy: halo — galaxies: dwarf — stars: abundances — stars: neutron

1. INTRODUCTION

The astrophysical origin of the rapid neutron-capture (r -process) elements is still unknown. Recent spectroscopic studies of Galactic halo stars have revealed the presence of Eu (almost pure r -process element in the solar system) in the atmospheres of extremely metal-poor (EMP) stars down to $[\text{Fe}/\text{H}] \sim -3$ with a large star-to-star scatter in $[\text{Eu}/\text{Fe}]$ (more than 2 orders of magnitude, e.g., Honda et al. 2004; François et al. 2007; Sneden et al. 2008). These observational features are reasonably reproduced by models of *inhomogeneous* Galactic chemical evolution (GCE), where a limited mass range (e.g., $8 - 10 M_\odot$) of core-collapse supernovae (CCSNe) is assumed to be the dominant source of the r -process elements (Ishimaru & Wanajo 1999; Tsujimoto, Shigeyama, & Yoshii 2000; Ishimaru et al. 2004; Argast et al. 2004). Previous *homogeneous* GCE models that assume a well-mixed, one-zone Galactic halo also suggest the low-mass end of CCSNe as the major r -process site (Mathews et al. 1992; Travaglio et al. 1999) but are not capable of accounting for the star-to-star scatter in $[\text{Eu}/\text{Fe}]$.

To date, however, no study of CCSN nucleosynthesis satisfactorily accounts for the production of heavy r -

process elements (see, e.g., Wanajo et al. 2011; Wanajo 2013). As an alternative scenario, binary mergers of double neutron stars (NSMs) as well as of neutron star–black hole pairs have long been suggested to be the r -process sites (Lattimer & Schramm 1974, 1976; Lattimer et al. 1977; Symbalisty & Schramm 1982; Eichler et al. 1989; Meyer 1989). In fact, a number of recent nucleosynthesis studies based on hydrodynamical simulations support NSMs to be the promising sources of r -process elements in the Galaxy (Freiburghaus et al. 1999; Goriely et al. 2011; Korobkin et al. 2012; Bauswein et al. 2013; Rosswog et al. 2014; Wanajo et al. 2014).

Recent GCE models appear to disfavor the NSM scenario except for the cases invoking very short lifetimes of neutron star binaries (1–10 Myr, Argast et al. 2004; De Donder & Vanbeveren 2004; Matteucci et al. 2014; Komiya et al. 2014; Tsujimoto & Shigeyama 2014; van de Voort et al. 2015; Wehmeyer et al. 2015)⁵. Estimates of binary lifetimes, $t_{\text{NSM}} \sim 0.1\text{--}1$ Gyr (e.g., Dominik et al. 2012), are in conflict with the presence of r -process-enhanced stars below $[\text{Fe}/\text{H}] \sim -2.5$ in those models. Even if a short-lived channel with $t_{\text{NSM}} \sim 1$ Myr exists (Belczynski & Kalogera 2001; De Donder & Vanbeveren 2004), the low Galactic rate of such events ($0.4\text{--}77.4 \text{ Myr}^{-1}$, Dominik et al. 2012) leads to a too large star-to-star scatter in $[\text{Eu}/\text{Fe}]$ at $[\text{Fe}/\text{H}] \gtrsim -2.5$ (Qian 2000; Argast et al. 2004). It should be noted, however, that the inhomogeneous GCE model of Argast et al. (2004) also appears to be in conflict with the observed small scatter of α elements relative to iron (Argast et al. 2002). This problem would be cured if the

¹ Department of Material Science, International Christian University, 3-10-2 Osawa, Mitaka, Tokyo 181-8585, Japan; ishmaru@icu.ac.jp

² iTHES Research Group, RIKEN, 2-1 Hirosawa, Wako, Saitama 351-0198, Japan; shinya.wanajo@riken.jp

³ Institut d’Astrophysique de Paris, UMR7095 CNRS, Univ. P. & M. Curie, 98bis Bd. Arago, 75104 Paris, France; prantzos@iap.fr

⁴ $[A/B] \equiv \log(N_A/N_B) - \log(N_A/N_B)_\odot$, where N_A indicates the abundance of A .

⁵ Note that the higher resolution model of van de Voort et al. (2015) also suggests short lifetimes of neutron star binaries.

TABLE 1
MODELS OF SUB-HALOS FOR CASES 1,2

M_* (M_\odot)	η	k_{OF} (Gyr^{-1})		k_{SF} (Gyr^{-1})	
		Case 1	Case 2	Case 1	Case 2
10^4	79	1.0	16	0.013	0.20
10^5	40	1.0	7.9	0.025	0.20
10^6	20	1.0	4.0	0.050	0.20
10^7	10	1.0	2.0	0.10	0.20
10^8	5.0	1.0	1.0	0.20	0.20
2×10^8	4.1	1.0	0.81	0.25	0.20

inhomogeneity of the inter-stellar medium (ISM) were modest because of effective matter mixing (or if more massive CCSNe had greater iron yields, Wehmeyer et al. 2015).

It should be noted that the aforementioned GCE models assume a single halo system (except for Komiya et al. 2014; van de Voort et al. 2015), which is incompatible with the currently dominant paradigm of the hierarchical merging scenario for galaxy formation. Prantzos (2006, 2008) has shown that the overall shape of the Galactic halo’s metallicity distribution (MD) can be well reproduced by a merging sub-halo model, with smaller sub-halos having suffered larger outflows (see also Komiya 2011). More importantly for the issue of r -process, Prantzos (2006) showed that if the sub-halos evolved at different rates, there would be no more a unique relation between time and metallicity; in that case, he argued that the observed “early” (in terms of metallicity) appearance of r -elements and their large dispersion can be explained, even if the main source of those elements is NSMs.

In this Letter, we study the role of NSMs in the early Galaxy with a GCE model based on the framework of such a hierarchical merging scenario and on recent estimates of the progenitor binary lifetimes.

2. CHEMICAL EVOLUTION OF SUB-HALOS

Each sub-halo is modeled as a one-zone, well-mixed single system that is losing gas by outflow (because of stellar winds, SN explosions and tidal interactions). The GCE model used in this work is the same as that of the ISM evolution of the Galactic halo in Ishimaru & Wanajo (1999); Ishimaru et al. (2004); Wanajo & Ishimaru (2006) but it differs in what follows. Each sub-halo is composed of stars with final total stellar mass M_* , evolving homogeneously (i.e., with its ISM well mixed at every time). We consider sub-halos with $M_*/M_\odot = 10^4, 10^5, 10^6, 10^7, 10^8$, and 2×10^8 . The heaviest mass is set to be about half the estimated stellar mass of the Galactic halo, $\sim 4 \times 10^8 M_\odot$ (Bell et al. 2008). The lowest mass corresponds to the one of recently discovered ultrafaint dwarf galaxies (Kirby et al. 2008).

Although we have no direct observational clues for the property of each sub-halo, recent observations of MDs of dwarf galaxies in the Local Group can provide some hints (Helmi et al. 2006). It is known that $[\text{Fe}/\text{H}]$ at the peak of a MD, $[\text{Fe}/\text{H}]_{\text{peak}}$, corresponds to effective yield y_{eff} , i.e., the iron productivity of a galaxy system which depends on the adopted stellar yields and IMF (Helmi et al. 2006; Prantzos 2008). If a dwarf galaxy loses a significant amount of iron through outflow with the rate (OFR) proportional to the star formation rate

TABLE 2
PARAMETERS ADOPTED FOR NSMS

Type	t_{NSM} (Myr)	$f_{\text{NSM}}/f_{\text{CCSN}}$	$M_{\text{Eu,NSM}}$ (M_\odot)
short-lived	1.00	1.0×10^{-4}	2×10^{-5}
long-lived	100	1.9×10^{-3}	2×10^{-5}

(SFR), y_{eff} is approximately proportional to η^{-1} , where $\text{OFR} \equiv \eta \text{SFR}$ (Prantzos 2008). In practice, limited data of MDs are available and thus the observed median metallicities ($[\text{Fe}/\text{H}]_0$) of dwarf galaxies are used instead of $[\text{Fe}/\text{H}]_{\text{peak}}$. Observed mass-metallicity relation of dwarf galaxies suggests that $[\text{Fe}/\text{H}]_0$ approximately scales as $M_*^{0.3}$ (Kirby et al. 2013). We thus assume $y_{\text{eff}}^{-1} \propto \eta = 5.0 (M_*/10^8 M_\odot)^{-0.3}$ as in Prantzos (2008)⁶. This can be naturally interpreted as a result of smaller SFR and/or greater OFR because of the shallower gravitational well for a less massive sub-halo (see also §4). SFR is assumed to be proportional to the mass of ISM (M_{ISM}): $\text{SFR} = k_{\text{SF}} M_{\text{ISM}}$, where the constant k_{SF} corresponds to the star formation efficiency, and $\text{OFR} = k_{\text{OF}} M_{\text{ISM}}$ as well, where $k_{\text{OF}} = \eta k_{\text{SF}}$. However, we cannot constrain either of k_{SF} or k_{OF} from observations. Thus, we assume two extremes: Cases 1 and 2 for the fixed ratios of η , respectively (Table 1). The sub-halo of $M_* = 10^8 M_\odot$ is (arbitrary) set to have the same values of k_{SF} and k_{OF} for both Cases 1 and 2.

The CCSN abundances of Mg and Fe (which we assume to be representative of CCSN products and metallicity, respectively) are taken from Nomoto et al. (2006). We ignore the Fe contribution from Type Ia SNe, because they appear to have played negligible role during the Milky Way halo evolution (the observed α/Fe ratio of halo stars is \sim constant). The evolution of each sub-halo is computed up to 2 Gyr, which is considered a reasonable estimate of the time-scale of the Milky Way halo formation suggested from the observed ages of globular clusters (Roediger et al. 2014). The value of k_{SF} for the sub-halo with $M_* = 10^8 M_\odot$ is set to account for the most metal rich stars in the Galactic halo.

Binary population synthesis models indicate an average binary lifetime of $\langle t_{\text{NSM}} \rangle \sim 1$ Gyr (e.g., Dominik et al. 2012), being comparable with the lifetimes of sub-halos. A significant fraction of NSMs are, however, expected to have $t_{\text{NSM}} \lesssim 100$ Myr ($\sim 40\%$, Belczynski et al. 2008). In addition, a short-lived channel of $t_{\text{NSM}} \lesssim 1$ Myr is also predicted (Belczynski & Kalogera 2001; Belczynski et al. 2002; De Donder & Vanbeveren 2004). Dominik et al. (2012) estimate the fraction of such a putative short-lived channel to be up to $\sim 7\%$ (for the solar metallicity case). For illustrative purposes, we assume here a bimodal distribution of $t_{\text{NSM}} = 1$ Myr and 100 Myr and with the corresponding fractions of 5% and 95%, respectively (Table 2). For the total average frequency of NSMs (f_{NSM}) relative to that of CCSNe we assume $\langle f_{\text{NSM}} \rangle = 2 \times 10^{-3} \langle f_{\text{CCSN}} \rangle$ adopting the estimates of the recent population synthesis calculations (Dominik et al. 2012). The mass of the ejected Eu, representative of

⁶ The values of the coefficient and the index are updated from Prantzos (2008) by adopting the latest mass-metallicity relation (Kirby et al. 2013).

TABLE 3
RESULTS RELATED TO MDs OF SUB-HALOS

M_* (M_\odot)	M_D (M_\odot)		[Fe/H] _{peak}	
	Case 1	Case 2	Case 1	Case 2
10^4	7.6×10^6	6.6×10^6	-2.63	-2.56
10^5	3.8×10^7	3.3×10^7	-2.33	-2.30
10^6	1.9×10^8	1.7×10^8	-2.03	-2.02
10^7	1.0×10^9	9.0×10^8	-1.74	-1.74
10^8	5.3×10^9	5.3×10^9	-1.46	-1.46
2×10^8	8.8×10^9	9.3×10^9	-1.38	-1.39

r -process elements in the Galactic halo, is taken from the latest nucleosynthesis result of Wanajo et al. (2014), $M_{\text{Eu,NSM}} = 2 \times 10^{-5} M_\odot$ (see also Goriely et al. 2011; Korobkin et al. 2012). The mass of the ejected Ba, which is also predominantly produced by the r -process in the early Galaxy, is set to be $M_{\text{Ba,NSM}} = 9 M_{\text{Eu,NSM}}$ according to the solar r -process ratio of these elements (Borris et al. 2000).

3. ENRICHMENT OF r -PROCESS ELEMENTS

Our results for Case 1 (with constant k_{OF}) are shown in Figure 1. Those results for less (more) massive sub-halos are indicated by the thinner (thicker) curves. The cumulative number of CCSNe in each sub-halo monotonically increases with time (Figure 1a). For NSMs, the cumulative number steeply rises when the long-lived binaries start contributing at 100 Myr. [Fe/H] monotonically increases with time for all the sub-halos; at a given time [Fe/H] is greater for more massive sub-halos because of their higher k_{SF} . MDs for all the sub-halos are also shown in Figure 1c. The metallicity at the peak of each MD, [Fe/H]_{peak} (Table 3), is in agreement with the observed mass-metallicity relation (Kirby et al. 2013) scaled downward by -0.4 dex to exclude SNe Ia contribution. The dark halo mass of each sub-halo, M_D (Table 3), estimated from the initial baryonic mass and the initial baryon to dark mass ratio (which is assumed to be equal to the cosmic value $\Omega_B/\Omega_D = 0.046/0.24 \sim 0.19$) implies $M_D \propto M_*^{0.7}$. Since the reasonable mass function of M_D can be regarded as $dN/dM_D \propto M_D^{-2}$ (e.g., Prantzos 2008, and the references therein), we obtain the sub-halo mass function as $\propto M_*^{-1.7}$. We find that the total MD (thick-black curve) weighted with the sub-halo mass function is in reasonable agreement with the observed one (gray-hatched region, An et al. 2013). We also find that the evolution of Mg (Figure 1d, representative of CCSN products) is in reasonable agreement with the observed stellar abundances of Galactic halo stars. In contrast to r -process elements, the observed scatters in $[\alpha/\text{Fe}]$ is known to be as small as the measurement errors (e.g., Cayrel et al. 2004). This result is consistent with such small scatters in $[\text{Mg}/\text{Fe}]$, because each evolutionary trend is almost independent of M_* .

The resulting evolution of Eu (representative of r -process elements) is presented in Figure 1e and compared to observed stellar values. We notice a transition from slow to rapid evolution of [Eu/Fe] for each sub-halo at ~ 100 Myr, as a result of the contribution from long-lived binaries starting. The corresponding [Fe/H] (see Figure 1b) differs from one sub-halo to another, being lower than [Fe/H] ~ -3 for $M_* \leq 10^6 M_\odot$. This in-

dicates that the presence of stars at [Fe/H] ~ -3 with star-to-star scatter in [Eu/Fe] ($\lesssim 0.5$) can be interpreted as a result of NSM activity in sub-halos with various k_{SF} . Our model cannot, however, explain the presence of r -process-enhanced stars with [Eu/Fe] > 1 . In addition our result predicts the presence of stars having [Eu/Fe] ~ -1 for [Fe/H] $\lesssim -3$. This is due to the contribution of the short-lived NSM at early times (< 100 Myr). Measurements of Eu in such stars would be challenging because of the weak spectral lines. Such a signature has been seen in the Ba abundances of EMP stars, [Ba/Fe] $\sim -2 - -1$ at [Fe/H] $\lesssim -3$ (Figure 1f), which could also be explained as due to the contribution of short-lived binaries. Note that the [Ba/Fe] values for [Fe/H] $\gtrsim -2.5$ are underpredicted compared to the observed ones; in this metallicity, contribution from the s -process becomes important (Borris et al. 2000).

Figure 2 shows the results for Case 2, where a constant k_{SF} is assumed. We find the cumulative numbers of NSMs and CCSNe being similar to those in Case 1 (Figure 1a). However, the evolutions stop earlier for less massive sub-halos. This is due to the termination of star formation because of gas removal by their significant outflows with greater values of k_{OF} . In contrast to Case 1, the [Fe/H] evolution (Figure 2b) is identical among sub-halos because of the same k_{SF} , although the termination points differ depending on their k_{OF} . The resulting MDs (Figure 2c) as well as the evolutions of Mg (Figure 2d) are similar between Cases 1 and 2. In Figure 2e, we find that the r -process abundances increase to values greater than [Eu/Fe] ~ 1 for the sub-halos with $M_* \leq 10^5 M_\odot$. This is a consequence of the fact that the higher k_{OF} lead to smaller Fe amounts and thus higher Eu/Fe ratios. It is interesting to note that, even without invoking inhomogeneity of ISM, the enhancement of Eu can be in part explained by our sub-halo models. However, our result here cannot account for the r -process enrichment at [Fe/H] ~ -3 because the [Eu/Fe]’s start rising at [Fe/H] ~ -2.4 for all the sub-halos.

Our results imply that the reality may be between these two extremes, Cases 1 and 2; reasonable combinations of k_{SF} and k_{OF} might account for the presence of r -process-enhanced stars at [Fe/H] ~ -3 . It is also important to note that the cumulative numbers for the least massive sub-halos ($M_* = 10^4 M_\odot$) are ~ 0.1 around the end of their evolutions. This could be another source of large enhancements of [Eu/Fe] ($\gtrsim 1$). The [Eu/Fe] values would be substantially higher than the *averaged* curves of our models, provided that only a fraction of sub-halos experienced NSMs.

4. SUMMARY AND DISCUSSION

We studied the role of NSMs for the chemical evolution of r -process elements in the framework of the Galactic halo formation from merging sub-halos. It is found that the appearance of Eu at [Fe/H] ~ -3 with star-to-star scatter in [Eu/Fe] ($\lesssim 0.5$) at [Fe/H] ~ -3 can be interpreted as a result of lower star formation efficiency k_{SF} for less massive sub-halos. On the other hand, the presence of highly r -process-enhanced EMP stars ([Eu/Fe] $\gtrsim 0.5$) can be explained if values of k_{OF} (the multiplicative factor for the outflow rate) are higher for less massive sub-halos. These may be reasonable assumptions because less massive sub-halo systems have weaker gravita-

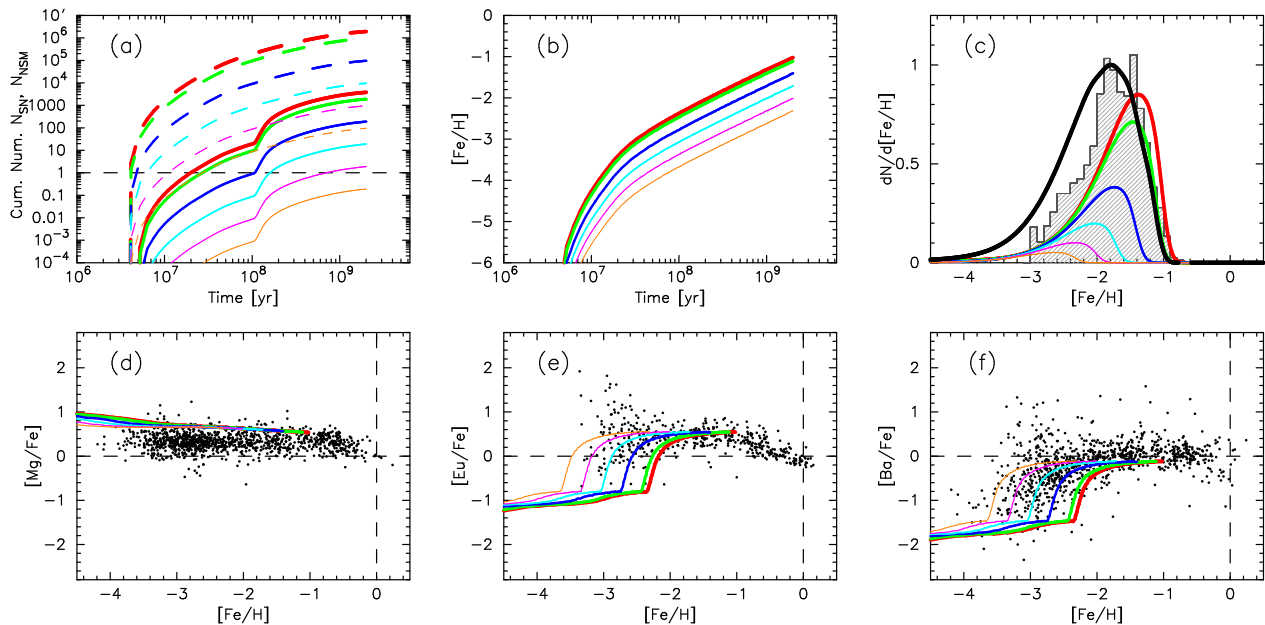


FIG. 1.— Evolution of the sub-halos with $M_*/M_\odot = 10^4, 10^5, 10^6, 10^7, 10^8,$ and 2×10^8 , respectively, indicated by the thinnest to thickest curves for Case 1. (a) Cumulative numbers of NSMs (solid) and CCSNe (dashed) as functions of time. The horizontal dashed line marks the number of unity (see text for implications). (b) [Fe/H] temporal evolutions. (c) MDs of sub-halos weighted with the sub-halo mass function and their sum (thick-black). Observational data of the Galactic halo (gray-hatched histogram) are taken from the calibration catalog of An et al. (2013). (d)-(f) [Mg/Fe], [Eu/Fe], and [Ba/Fe] as functions of [Fe/H], respectively. The horizontal and vertical lines indicate the solar values. Observational stellar values (dots) are taken from the SAGA database (Suda et al. 2008), excluding carbon-enhanced stars that may have been affected by gas transfer in binaries.

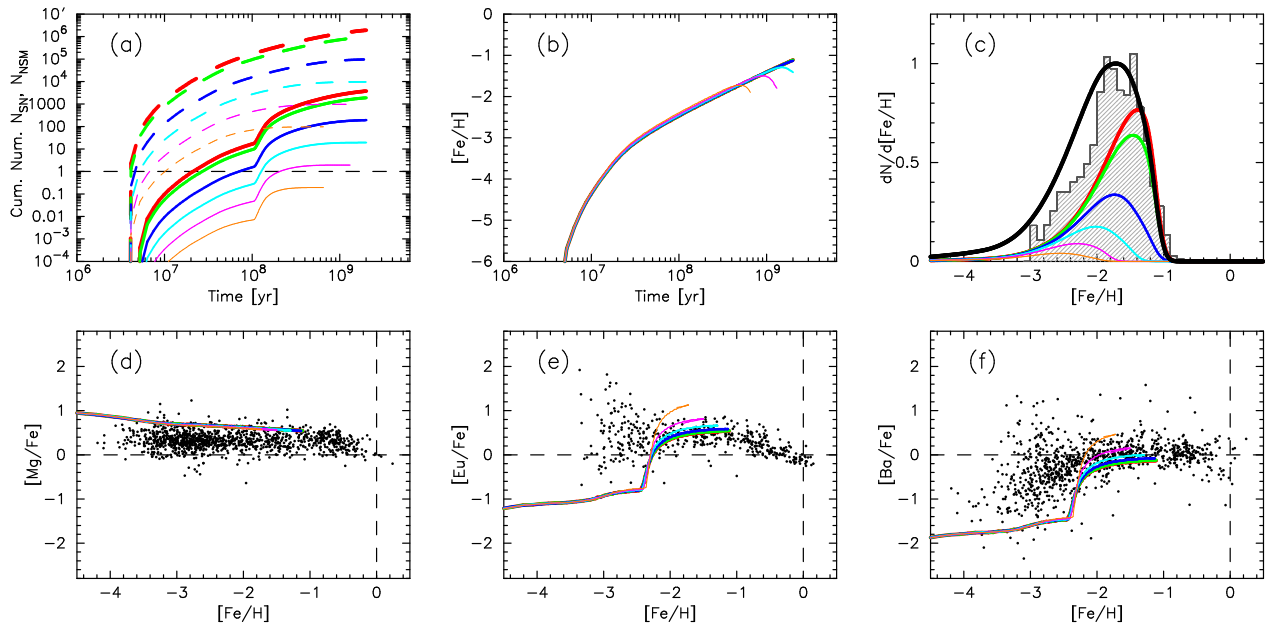


FIG. 2.— Same as Figure 1, but for Case 2.

tional potential (as indicated by M_D in Table 3) and thus are expected to form stars less efficiently and/or expel the ISM more easily. The ratio of OFR to SFR, η , is assumed to be proportional to $M_*^{-0.3}$. Recent observations of relatively massive galaxies ($10^7 - 10^{11} M_\odot$) also suggest similar anti-correlation between M_* and η (Chisholm et al. 2014). Under this assumption, the metallicity at the peak of each sub-halo’s MD (Table 3) appears to be consistent with the observed mass-metallicity relation. In

addition, the total MD weighted with the sub-halo mass function shows reasonable agreement with the observed one of the Galactic halo.

The low-level Ba abundances ($[Ba/Fe] \sim -1.5$) observed in the EMP stars of $[Fe/H] \lesssim -3$ may be due to the contribution from the short-lived binaries (with $t_{NSM} = 1$ Myr in this study). Thus, the main features of r -process abundances observed in EMP stars, their appearance at $[Fe/H] \sim -3$ with large star-to-star scat-

ter and their sub-solar amounts for $[\text{Fe}/\text{H}] \lesssim -3$, can be potentially explained by the contribution from solely NSMs.

The highly Eu enhanced stars at $[\text{Fe}/\text{H}] \sim -3$ may be accounted by reasonable combinations of k_{SF} and k_{OF} . The small cumulative numbers of NSMs (< 1) for least-massive sub-halos could be additional reason for the observed large scatter in $[\text{Eu}/\text{Fe}]$, because NSMs may occur only in some of them, while no NSMs occur in others. Once NSMs occur in such less massive systems, their ISM must be highly enriched by r -process elements.

In conclusion, our results imply that the current observational evidences of r -process signatures in EMP stars can be interpreted as a consequence of the Galactic halo formation from merging sub-halos. If the model is a reasonable simplification for such chemo-dynamical evolutions of sub-halos, NSMs can be the main r -process contributors throughout the Galactic history. Contribu-

tions from CCSNe are not necessarily needed as invoked in previous GCE studies. Note that our assumption of well-mixed ISM might not necessarily be an oversimplification, at least for less-massive sub-halos, in which a small number of explosive events would easily homogenize their smaller amount of ISM before the next episode of star formation. The observed small scatters of abundance ratios of other elements such as iron-peak elements or α -elements in EMP stars should be examined using a consistent assumption. Possible effects of ISM inhomogeneity as well as of stochastic nature of NSM events (i.e., $N_{\text{NSM}} < 1$) will be discussed in a forthcoming paper.

This work was supported by the RIKEN iTHES Project and the JSPS Grants-in-Aid for Scientific Research (26400232, 26400237).

REFERENCES

- An, D., Beers, T. C., Johnson, J. A., et al. 2013, *ApJ*, 763, 65
 Argast, D., Samland, M., Thielemann, F.-K., Gerhard, O. E. 2002, *A&A*, 388, 842
 Argast, D., Samland, M., Thielemann, F.-K., & Qian, Y.-Z. 2004, *A&A*, 416, 997
 Bauswein, A., Goriely, S., & Janka, H.-T. 2013, *ApJ*, 773, 78
 Belczynski, K. & Kalogera, V. 2001, *ApJL*, 550, L183
 Belczynski, K., Kalogera, V., & Bulik, T. 2002, *ApJ*, 572, 407
 Belczynski, K., Kalogera, V., Rasio, F. A., Taam, R. E., et al. 2008, *ApJS*, 174, 223
 Bell, E., Zuker, D., Belokurov, V. et al., 2008, *ApJ*, 680, 295
 Burris, D. L., Pilachowski, C. A., Armandroff, T. E., Sneden, C., Cowan, J. J., & Roe, H. 2000, *ApJ*, 544, 302
 Cayrel, R., et al. 2004, *A&A*, 416, 1117
 Chisholm, J., Tremonti, C. A., Leitherer, C., Chen, Y., Wofford, A., & Lundgren, B. 2014; arXiv:1412.2139
 De Donder, E. & Vanbeveren, D. 2004, *New Astron. Rev.*, 48, 861
 Dominik, M., Belczynski, K., Fryer, C., et al. 2012, *ApJ*, 759, 52
 Eichler, D., Livio, M., Piran, T., & Schramm, D. N. 1989, *Natur*, 340, 126
 François, P., et al. 2007, *A&A*, 476, 935
 Freiburghaus, C., Rosswog, S., & Thielemann, F.-K. 1999, *ApJ*, 525, L121
 Goriely, S., Bauswein, A., & Janka, H.-T. 2011, *ApJ*, 738, L32
 Helmi, A., Irwin, M., Tolstoy, E., et al. 2006, *ApJL*, 651, L121
 Honda, S., et al. 2004, *ApJ*, 607, 474
 Ishimaru, Y. & Wanajo, S. 1999, *ApJL*, 511, L33
 Ishimaru, Y., Wanajo, S., Aoki, W., & Ryan, S. G. 2004, *ApJ*, 600, L47
 Kirby, E. N., Simon, J. D., Geha, M., Guhathakurta, P., & Frebel, A. 2008, *ApJL*, 685, L43
 Kirby, E. N., Cohen, J. G., Guhathakurta, P., Cheng, L., & Bullock, J. S., 2013, *ApJ*, 779, 102
 Komiya, Y. 2011, *ApJ*, 736, 73
 Komiya, Y., Yamada, S., Suda, T., & Fujimoto, M. Y. 2014, *ApJ*, 783, 132
 Korobkin, O., Rosswog, S., Arcones, A., & Winteler, C. 2012, *MNRAS*, 426, 1940
 Lattimer, J. M. & Schramm, D. N. 1974, *ApJ*, 192, L145
 Lattimer, J. M. & Schramm, D. N. 1976, *ApJ*, 210, 549
 Lattimer, J. M., Mackie, F., Ravenhall, D. G., & Schramm, D. N. 1977, *ApJ*, 213, 225
 Mathews, G. J., Bazan, G., & Cowan, J. J. 1992, *ApJ*, 391, 719
 Matteucci, F., Romano, D., Arcones, A., Korobkin, O., & Rosswog, S. 2014, *MNRAS*, 438, 2177
 Meyer, B. S. 1989, *ApJ*, 343, 254
 Nomoto, K., Tominaga, N., Umeda, H., Kobayashi, C., Maeda, K., 2006, *Nucl. Phys. A*, 777, 424
 Prantzos, N. 2006, in *Proceedings of the International Symposium on Nuclear Astrophysics - Nuclei in the Cosmos - IX*. 25-30 June 2006, CERN., p.254.1
 Prantzos, N. 2008, *A&A*, 489, 525
 Qian, Y.-Z. 2000, *ApJL*, 534, L67
 Roediger, J. C., Courteau, S., Graves, G., Schiavon, R. P. 2014 *ApJS*, 210, 10
 Rosswog, S., Korobkin, O., Arcones, A., Thielemann, F.-K., & Piran, T. 2014, *MNRAS*, 439, 744
 Sneden, C., Cowan, J. J., & Gallino, R. 2008, *ARAA*, 46, 241
 Suda, T., Katsuta, Y., Yamada, S., Suwa, T., Ishizuka, C., Komiya, Y., Sorai, K., Aikawa, M., & Fujimoto, M. Y., 2008, *PASJ*, 60, 1159
 Symbalisty, E., & Schramm, D. N. 1982, *ApL*, 22, 143
 Travaglio, C., Galli, D., Gallino, R., Busso, M., Ferrini, F., Straniero, O. 1999, *ApJ*, 521, 691
 Tsujimoto, T., Shigeyama, T., & Yoshii, Y. 2000, *ApJL*, L531, 33
 Tsujimoto, T. & Shigeyama, T. 2014, *A&A*, 565, L5
 van de Voort, F., Quataert, E., Hopkins, P. F., Kereš, D., & Faucher-Giguère, C.-A. 2015, *MNRAS*, 447, 140
 Wanajo, S. & Ishimaru, I. 2006, *Nucl. Phys. A*, 777, 676
 Wanajo, S., Janka, H.-T., & Müller, B. 2011, *ApJL*, 726, L15
 Wanajo, S. 2013, *ApJL*, 770, L22
 Wanajo, S., Sekiguchi, Y., Nishimura, N., Kiuchi, K., Kyutoku, K., & Shibata, M. 2014, *ApJL*, 789, L39
 Wehmeyer, B., Pignatari, M., & Thielemann, F.-K. 2015; arXiv:1501.07749